

Theoretical Study on the Interactions between Cellulose and Different Methyltriethoxysilane Hydrolysis Products

Tong Xing,^a Changqing Dong,^{a,b,*} Xiaoying Hu,^a Junjiao Zhang,^c Ying Zhao,^a Junjie Xue,^a and Xiaoqiang Wang^a

Silylation is an effective means of cellulose modification. However, the condensation reaction process between the hydrolysis products of the silane coupling agent and cellulose, as well as the structure of the coating, which both have a strong influence on the wettability, are still controversial. In this paper, the reactions of different methyltriethoxysilane hydrolysis products with cellulose were simulated *via* the density functional theory method. The reaction activity centers of the different methyltriethoxysilane hydrolysis products in an ethanol solution were analyzed *via* the front-line orbital theory and the Fukui function. The silylation reaction of different methyltriethoxysilane hydrolysis products in an ethanol solution on the cellulose surface were investigated *via* the transition state theory. The results show that although the initial hydrolysis product has the lowest grafting energy barrier, considering the whole process of grafting and condensation on the cellulose surface, the hydrolysis product with two hydroxyl groups is more favorable for the growth of organosilicon on the cellulose surface, so it is desirable to control the reaction where this product is dominant. In addition, the silylation process on the cellulose surface is more inclined to a multilayer coating mechanism.

DOI: 10.15376/biores.17.4.5728-5740

Keywords: Cellulose; Methyltriethoxysilane; Density functional theory; Grafting reaction

Contact information: a: National Engineering Laboratory for Biomass Power Generation Equipment, School of New Energy, North China Electric Power University, Beijing 102206 China; b: State Key Laboratory of Alternate Electrical Power System with Renewable Energy Sources, North China Electric Power University, Beijing 102206 China; c: School of Energy, Power and Mechanical Engineering, North China Electric Power University, Beijing 102206 China; *Corresponding author: dongcq@ncepu.edu.cn

INTRODUCTION

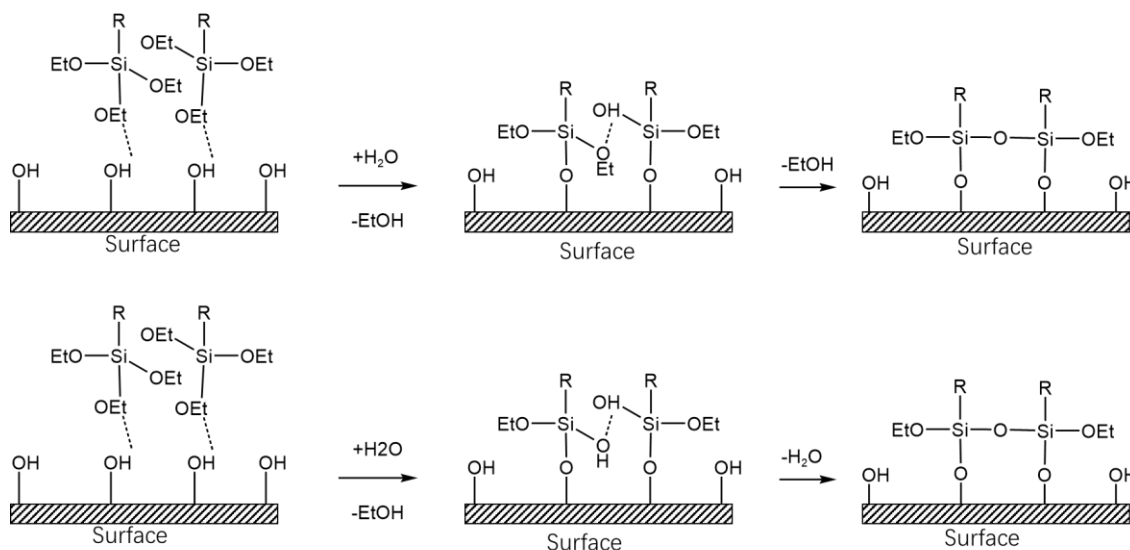
Cellulose is the most abundant biopolymer on Earth; it is found in trees, waste from agricultural crops, and other biomasses (Li *et al.* 2021). With multiple advantages, including a low cost, renewability, easy processability, and biodegradability, as well as appealing mechanical performance, dielectricity, piezoelectricity, and convertibility (Béguin and Aubert 1994; Zhao *et al.* 2021), cellulose is an emerging potential material in energy storage (Li *et al.* 2022), wastewater treatment (Chen *et al.* 2017), desalination (Zhu *et al.* 2017; Li *et al.* 2018), flexible materials (Zhu *et al.* 2016; Zhao *et al.* 2021), *etc.*

Cellulose nanotechnology has been developed to produce various structures, *e.g.*, super-strong wood, transparent wood, and cooling wood for lightweight and energy-efficient building applications (Chen *et al.* 2020), as well as fabric materials ranging from composites and macrofibres to thin films, porous membranes, and gels (Ye *et al.* 2019; Tu *et al.* 2021). However, there are disadvantages of cellulose, which is prone to water absorption and degradation, at the same time causing it easily to lose strength rapidly,

which limits its application in humid and aqueous environments.

Grafting hydrocarbon polymers on the surface of cellulose is an effective method to improve hydrophobicity (Xie *et al.* 2010). For example, cellulose aerogels modified by polysiloxane, such as polydimethylsiloxane (PDMS), can have a water contact angle of greater than 150° and can be used for oil-water separation (Wang *et al.* 2019; Phat *et al.* 2021). Alternatively, hydrophobic silanized cellulose can be produced by *in situ* polymerization of silane coupling agents on the cellulose surface to form polysiloxane networks (Wang *et al.* 2016). More importantly, silanization with silane coupling agents allows the formation of a micro-/nano morphology, which has a strong influence on the wettability (Liu *et al.* 2017; Feng *et al.* 2002). Therefore, in a previous work by the authors, a cellulose-based oil-water separation membrane with a water contact angle of 164.2° was prepared using silane coupling agents (Xing *et al.* 2022).

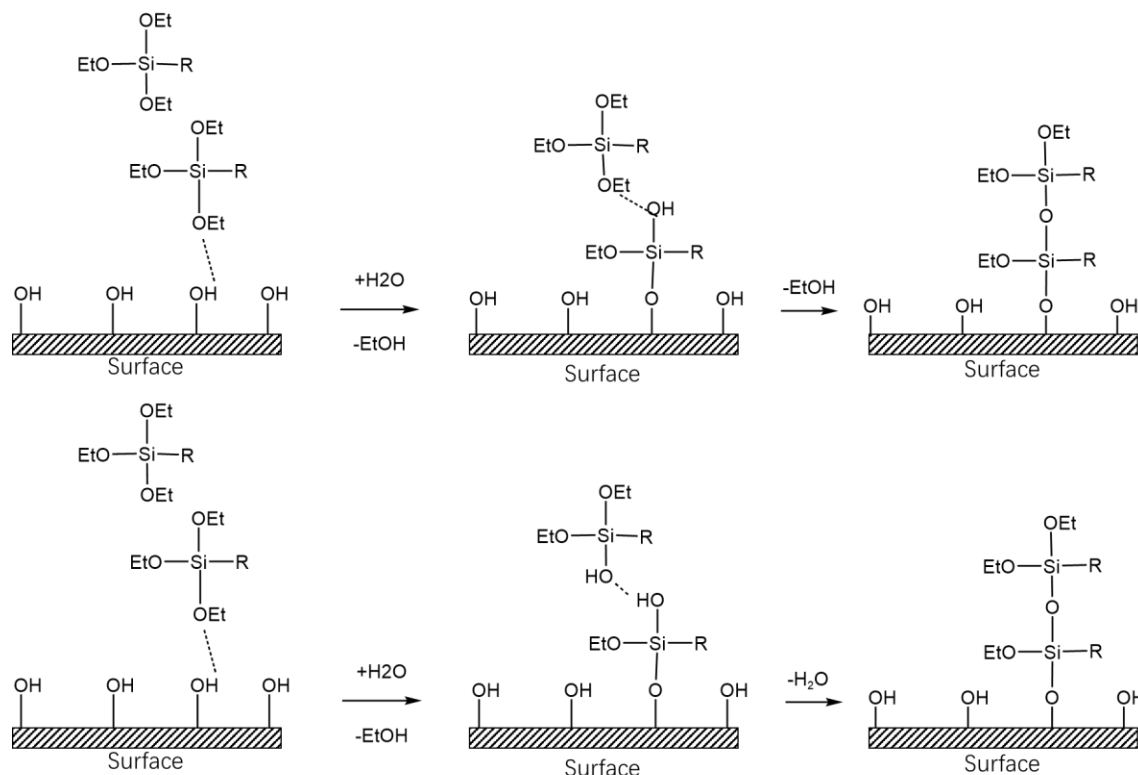
The coupling of silane on cellulose is generally accomplished in two stages. In the first step, the silane coupling agent is hydrolyzed to silanol, which is condensed with the OH groups on the cellulose in a subsequent step (Rana *et al.* 2021). However, the structure and properties of the coating are still controversial (Hunsche *et al.* 1997; Vilmin *et al.* 2014). So far, two conflicting theories for the silylation mechanism have been proposed. The generally accepted theory is called horizontal grafting (Xie *et al.* 2010, 2017) (Scheme 1), while the other one is called multilayer coating (Yoshida *et al.* 2001; Shircliff *et al.* 2013) (Scheme 2). It is not clear which one is favored by the condensation reaction process between the hydrolysis products of the silane coupling agent and the cellulose.



Scheme 1. Horizontal grafting mechanism. (R represents the organic functional group of silane; the dotted lines represent hydrogen bonds.)

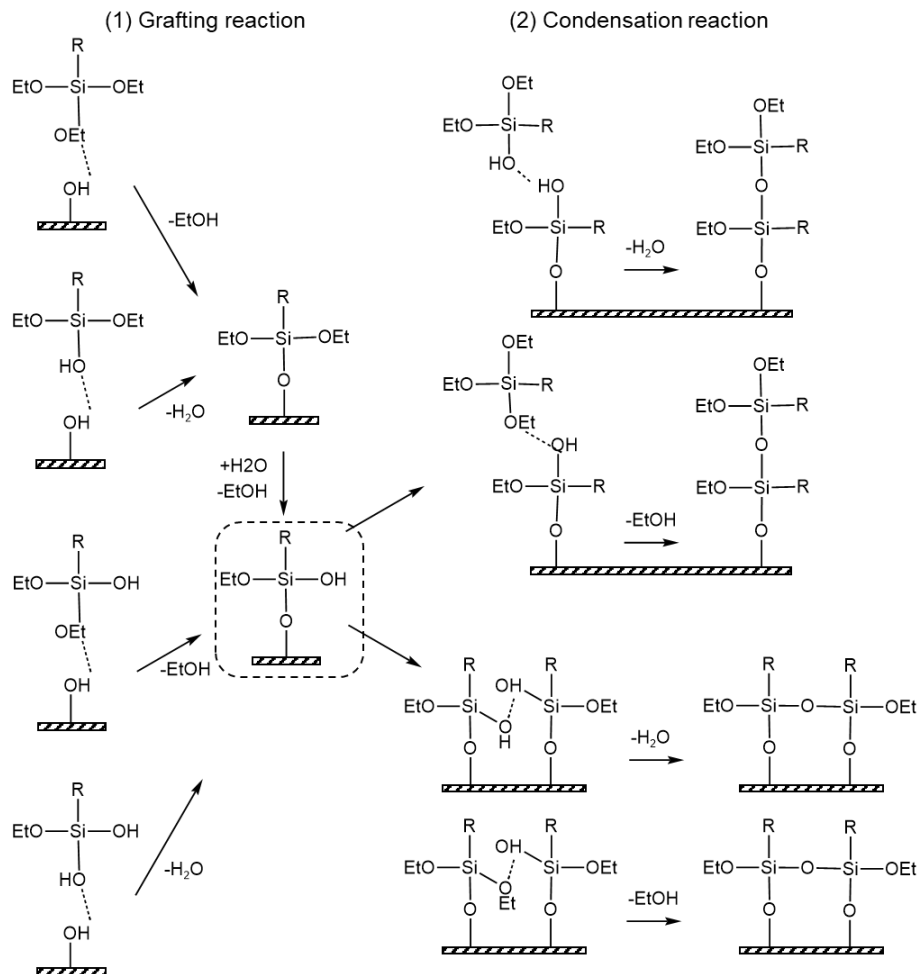
Shang and Zhang (2020) studied the interaction between silica and different 3-mercaptopropyltriethoxysilane (MPTS) hydrolysis products *via* Density Functional Theory (DFT) methods and tried to reveal the silylation mechanism. It was concluded that grafted silanes adsorbed flatly on the silica surface, and the elimination of ethanol promoted the grafting of partially hydrolyzed silane on the silica surface. However, the MPTS hydrolysis products adsorbed flatly on the surface of silica due to the influence of S atoms on the longer alkyl chains. In order to exclude the interference of the R group, the triethoxysilane

(MTES) with the R group being methyl, the most common hydrophobic group, is appropriate to study. And the theoretical calculations do not take into account the dipole electrostatic interaction between the solvent, *e.g.*, methanol (Liu *et al.* 2004), ethanol (Chen *et al.* 1996), and the reactants (Iarlori *et al.* 2001; Deetz *et al.* 2016), which is inconsistent with the fact that surface treatments are usually carried out in a silane water-alcohol solution (Salon *et al.* 2005). It is worth exploring whether the interaction, adsorption behavior, and reaction profiles of the hydrolysis products of silane coupling agents with cellulose in ethanol solutions are similar to the silica surface grafting mechanism.



Scheme 2. Multilayer coating mechanism

In order to investigate whether the process of MTES grafting on the cellulose surface prefers Scheme 1 or 2, the reaction process is viewed as two parts: grafting and condensation reaction. In this paper, the reaction scheme that goes through the most representative intermediate product containing only one hydroxyl group as an example (as shown in Scheme 3) is taken as an example. There are four main reaction schemes for the formation of the intermediate product, while there are two types of subsequent condensation reactions. The activation energies of grafting and condensation reactions in an ethanol solution were investigated based on the Density Functional Theory (DFT) method and the cellulose I β crystal model, revealing the effects of the solvent on the grafting reaction mechanisms. The hydrolysis product with two hydroxyl groups is predicted to be more favorable for the growth of organosilicon on the cellulose surface. In addition, the silylation process on the cellulose surface is more inclined to a multilayer coating mechanism.



Scheme 3. scheme that goes through the most representative intermediate product containing only one hydroxyl group

EXPERIMENTAL

Models

Natural cellulose has two different crystalline forms, $I\alpha$ and $I\beta$. The cellulose in wood is primarily cellulose $I\beta$ (as shown in Fig. 1) (Belton *et al.* 1989). The external morphology of cellulose $I\beta$ primarily corresponds to the (110) and (1 $\bar{1}0$) surfaces, which are highly decorated by protruding hydroxyls (Mazeau and Rivet 2008).

In the investigation of the adsorption and chemical reaction mechanisms, the cluster model can guarantee a high accuracy with low computational effort (Taylor *et al.* 2011). The chemical properties of the clusters differ from those of macroscopic cellulose fibers, exposing more active sites. Therefore, based on the analysis of the reaction centers, those with similarities to the crystals were chosen. In this paper, the cellulose $I\beta$ model was established based on the lattice structure data characterized by synchrotron X-ray and neutron diffraction, as shown in Nishiyama *et al.* (2003), and the cellulose cluster model isolated from the (110) crystal plane of cellulose $I\beta$ was chosen (as shown in Fig. 1c).

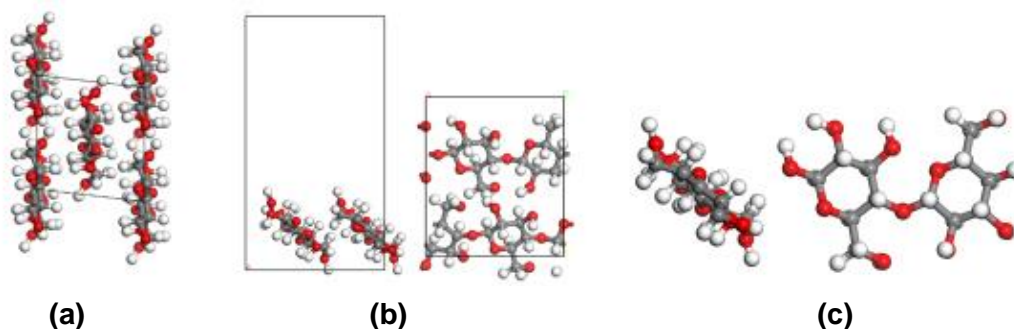


Fig. 1. The cellulose models: (a) cellulose I β ; (b) (100) surface of cellulose I β ; and (c) cellulose cluster model isolated from the (110) crystal plane of cellulose I β (note: the grey, white, red balls are for C, H, and O atoms, respectively)

Calculation Details

The primitive cellulose model was optimized using the Dmol³ program package (Delley 1990, 2000) in the Materials Studio software (version 5.5, BIOVIA, San Diego, CA). The generalized gradient approximation (GGA) developed by Perdew-Burke-Ernzerhof (PBE) (Perdew *et al.* 1996) was selected as the exchange-correlation function because of its high accuracy in terms of hydrogen bond description. The double numerical basis set plus polarization function (DNP) was used, and all electrons were considered without special core treatment. Under this calculation scheme, the basis set superposition error (BSSE) can be minimized (Delley 1990). The dispersion-corrected density functional theory (DFT-D) was employed to analyze the effects of the dispersion force.

The orbital truncation radius was set to 4.6 Å (1 Å = 0.1 nm), and the core treatment was set to all electron. The maximum energy change was 10⁻⁵ Ha, the maximum force was 0.002 HaÅ⁻¹, and the maximum displacement was 0.005 Å. The self-consistent field convergence was set as 10⁻⁶. The conductor-like screening model (COSMO) are used for reactions in solution and is set to ethanol (24.3) and the other calculations are in gas phase.

Different methyltriethoxysilane (MTES) hydrolysis products were optimized using the Dmol³ program package. The optimized structure was analyzed for the electron density, electrostatic potential, front-line orbitals, and Fukui functions.

The linear synchronous transit (LST)/quadratic synchronous transit (QST) method was used to search the transition state for each reaction. After vibrational analysis of reactants and products, whether they are transition states was confirmed according to the direction of the imaginary frequency vibration and its connectivity, and then optimize the transition state and frequency were optimized. The activation energy and heat of the reaction was calculated according to Eqs. 1 and 2, respectively,

$$E_A = E_{TS} - E_R \quad (1)$$

$$E_h = E_P - E_R \quad (2)$$

where E_A is the activation energy (kJ/mol), E_{TS} is the energy of the transition state (kJ/mol), E_R is the energy of the reactants (kJ/mol), E_h is the heat of the reaction (kJ/mol), and E_P is the energy of the products (kJ/mol).

RESULTS AND DISCUSSION

Activity Center Analysis

There are three types of MTES hydrolysis products (denoted by MH0): where one ethoxy group is hydrolyzed, where two ethoxy groups are hydrolyzed, and where all ethoxy groups are hydrolyzed, which are denoted by MH1, MH2, and MH3, respectively (Shang and Zhang 2020).

The activity of the grafting reaction can be quantified with the help of the front-line orbital electron clouds (as shown in Fig. 2) and the Fukui function (as shown in Fig. 3). The shift of the frontline orbitals makes the Si atom more electrophilic and the O atom more nucleophilic, thus increasing the activity (Yokoyama *et al.* 1999; Zhuo *et al.* 2012). The electrophilic indices of the Si atoms in MH0 through MH3 show a tendency to increase with the hydrolysis process, which is consistent with the substitution of -OEt by -OH, which is consistent with the literature (Liu *et al.* 2004). Hydrolysis makes the O atom readily accept the hydrogen atom in the hydroxyl group of cellulose, and the hydroxyl group in the hydrolysis product is more vulnerable to the attack of the hydroxyl group on the cellulose surface compared to the ethoxy group, which is considerably different from the literature reports that do not consider solubilization effects (Shang and Zhang 2020).

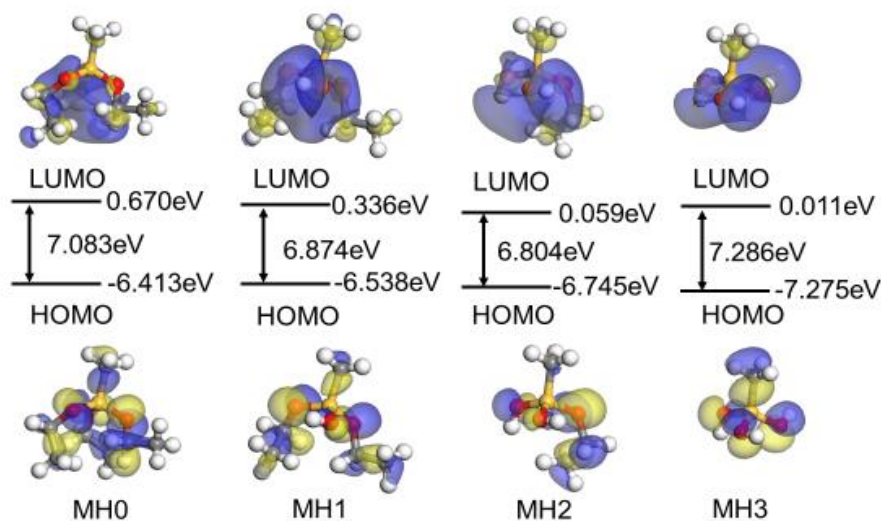


Fig. 2. The LUMOs and HOMOs of the MTES hydrolyzed products

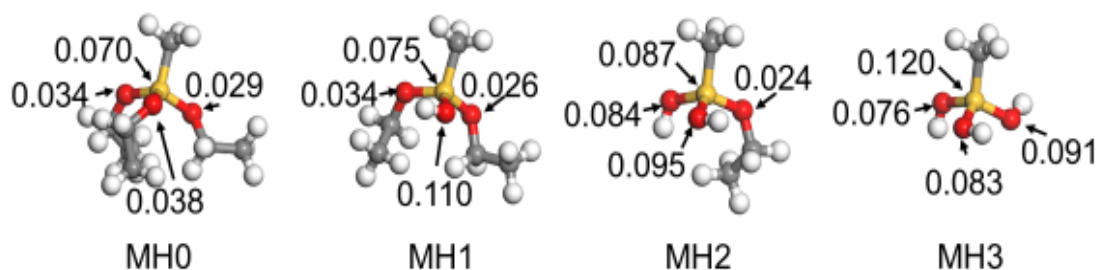


Fig. 3. Electrophilic index of Si and nucleophilic index of O in the MTES hydrolyzed products

Grafting And Condensation Reaction

Based on the above analysis of the reaction activity centers, the influence of the MTES hydrolysis process on the grafting and condensation reaction mechanism is revealed via kinetic calculations with the help of the transition state theory.

Grafting reaction between cellulose and different MTES hydrolysis products

The differences in the reaction mechanisms between alcohol and non-solvent environments were analyzed. The PES profile of the MH0 grafting reaction is shown in Fig. 4, and the reactant energy was set to 0 in kJ/mol. In an ethanol solvent, MH0 is first adsorbed on the cellulose surface as the hydrogen bond with a length of 2.204 Å. After that, the silica atom of MH0 is subjected to nucleophilic attack by the oxygen atom in the cellulose hydroxyl group. After the transition state, TS-MH0, with an activation energy of 22.9 kJ/mol, the silica atom of MH0 binds to the oxygen atom in the cellulose hydroxyl group with a length of 2.020 Å. Subsequently, the silica-oxygen bond in MH0 breaks, and the hydrogen atom in the cellulose hydroxyl group transfers and binds to the broken ethoxy group to form ethanol to complete the grafting, which is exothermic.

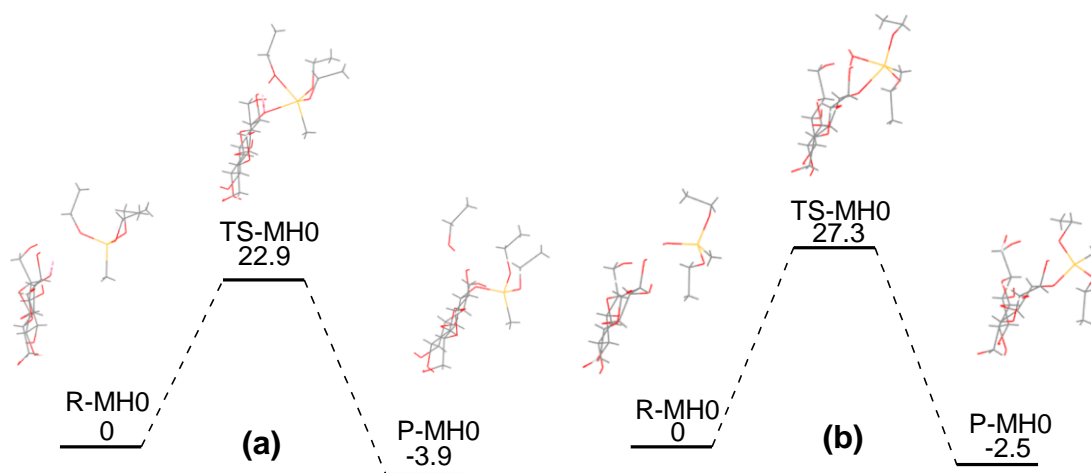


Fig. 4. The potential energy surface (PES) profile of the grafting reaction of MH0: (a) in ethanol; and (b) in gas phase

The incomplete hydrolysis product has both ethoxy and hydroxyl groups, so there are profiles of deethanolization and dehydration reactions (shown in Fig. 5 and 6). The PES curves of the reaction of the complete hydrolysis product MH3 are shown in Fig. 7. The deethanolization reaction activation energy in ethanol is higher than that of the grafting reaction of MH0 (22.9 kJ/mol). In addition, the activation energy of the dehydration reaction tends to be lower.

The PES profiles of the reactions in a non-solution show significant differences from those in an ethanol solution, especially for MH1. The activation energy of the deethanol profile in an ethanol solution is higher; while under non-solution conditions, the activation energy of the dehydration profile is higher, and the dehydration profile reaction is a slight heat absorption reaction.

The products of the incomplete hydrolysis of MTES prefer the dehydration profile in an ethanol solution, while the non-solution conditions prefer the deethanol profile. This is because of the fact that the oxygen atoms in the MH1 and MH2 silicone hydroxyl groups have higher nucleophilic properties compared to the ethoxy groups in an ethanol solution

and bind more strongly to the hydrogen atoms in cellulose, contrary to the properties in the non-solution environment (Shang and Zhang 2019).

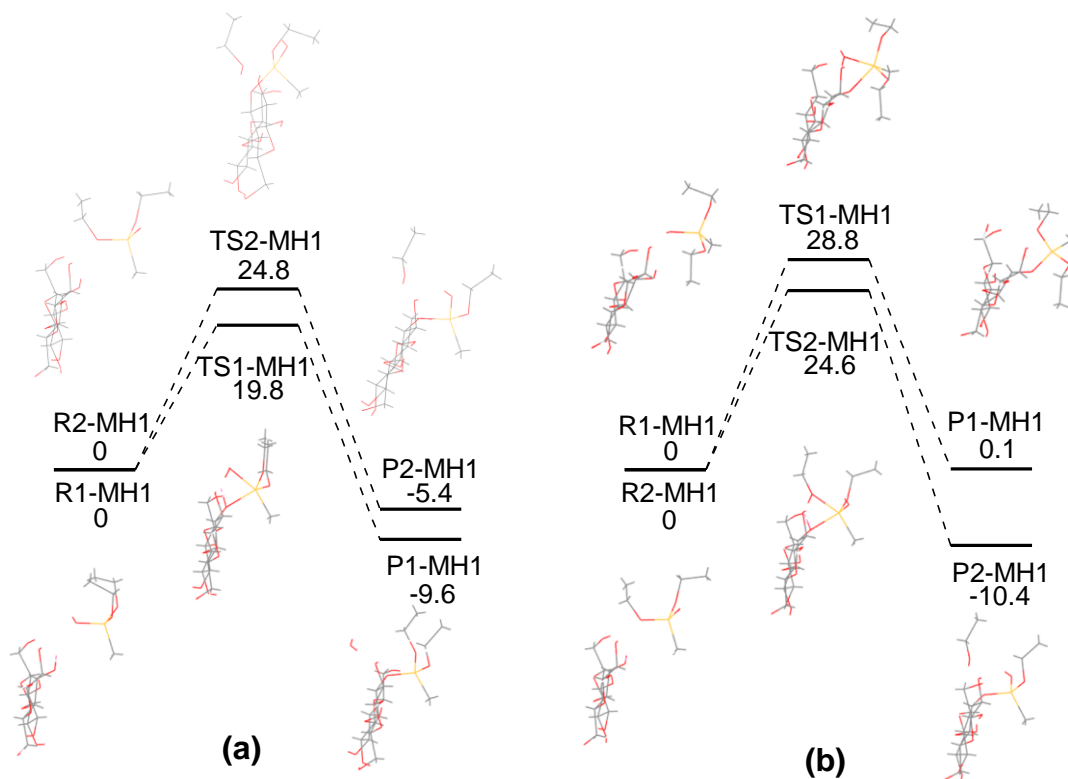


Fig. 5. The PES profile of the grafting reaction of MH1: (a) in ethanol; and (b) in gas phase

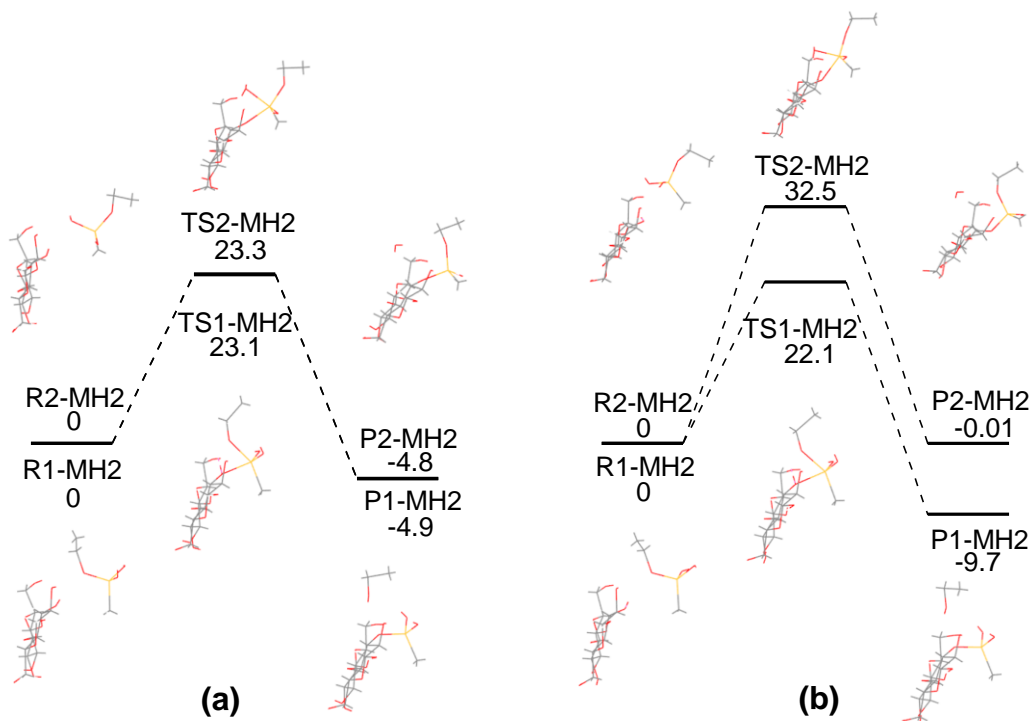


Fig. 6. The PES profile of the grafting reaction of MH2: (a) in ethanol; and (b) in gas phase

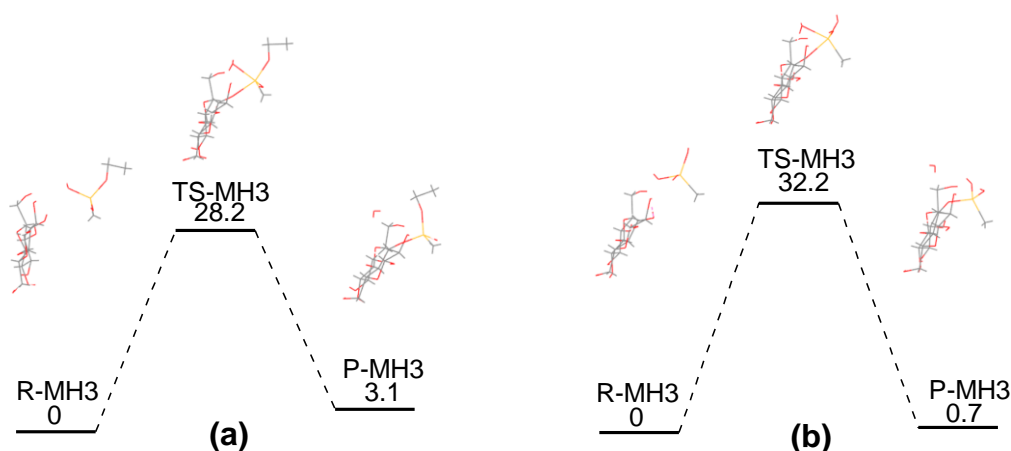


Fig. 7. The PES profile of the grafting reaction of MH3: (a) in ethanol; and (b) in gas phase

Grafting reaction

Intermediates containing only one hydroxyl group are representative intermediates for the grafting and condensation reactions of MTES and its hydrolysis products on the cellulose surface. The formation of representative intermediates requires a one- or two-step reaction, and there are four main cases. Among them, the dehydration grafting of MH2 on the cellulose surface has the lowest energy barrier (shown in Fig. 8).

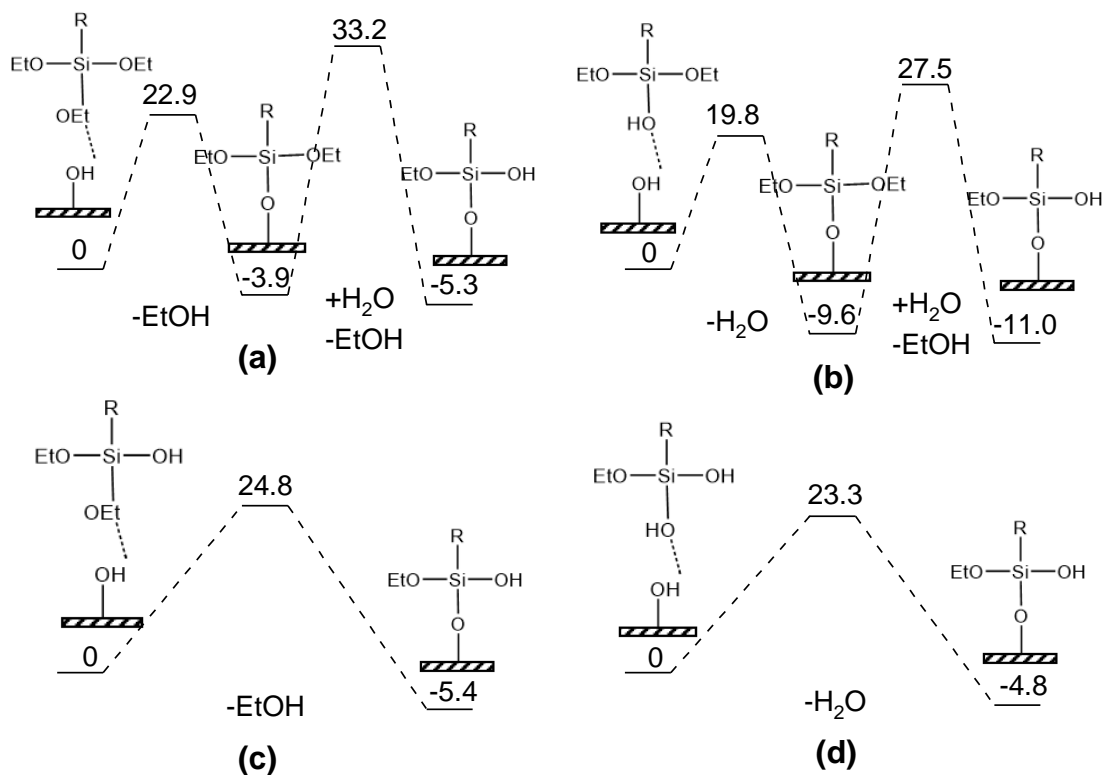


Fig. 8. The PES profile of the formation of representative intermediates: (a) MH0; (b) and (c) MH1; (d) MH2

Condensation reaction

The dehydration condensation reactions are shown between the intermediate products and the free MTES hydrolysis products in solution (in the case of the major hydrolysis product containing one hydroxyl group) or the intermediate products correspond to the most likely vertical growth (multilayer coating) and horizontal condensation (horizontal grafting) reactions, respectively. As shown in Fig. 9, the reaction energy barriers for multilayer coating and horizontal grafting are close, but the energy of the vertical growth product is significantly lower than that of the horizontal condensation product.

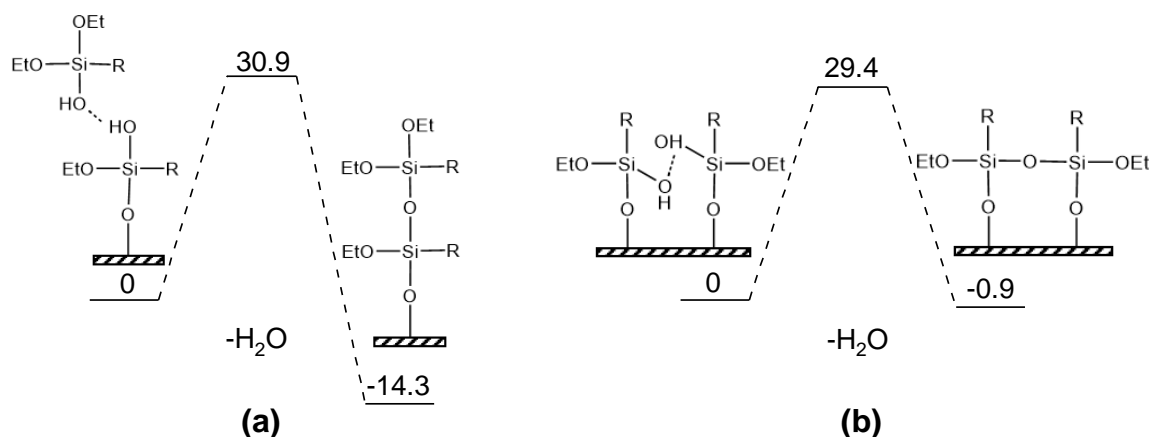


Fig. 9. The PES profile of the dehydration condensation reactions: (a) multilayer coating; and (b) horizontal grafting

Although the initial hydrolysis product has the lowest grafting energy barrier, considering the whole process of grafting and condensation on the cellulose surface, the hydrolysis product with two hydroxyl groups is more favorable for the growth of organosilicon on the cellulose surface, so it is desirable to control the reaction where this product is dominant. The silylation process on the cellulose surface also tends to be a multilayer coating mechanism.

CONCLUSIONS

1. The hydroxyl oxygen of the incompletely hydrolyzed products is more active in the ethanol solution environment, and therefore more likely to undergo condensation *via* a dehydration reaction.
2. Although the initial hydrolysis product has the lowest grafting energy barrier, considering the whole process of grafting and condensation on the cellulose surface, the hydrolysis product with two hydroxyl groups is more favorable for the growth of organosilicon on the cellulose surface.
3. The silylation process on the cellulose surface tends to be a multilayer coating mechanism.

ACKNOWLEDGMENTS

This work was financially supported by the Natural Science Foundation of China (Grant No. 51776070) and the State Grid Science and Technology Program (Grant No. SGGNSW00YWJS2100024).

REFERENCES CITED

- Béguin, P., and Aubert, J.-P. (1994). "The biological degradation of cellulose," *FEMS Microbiology Reviews* 13(1), 25-58. DOI: 10.1111/j.1574-6976.1994.tb00033.x
- Chen, S.-L., Dong, P., Yang, G.-H., and Yang, J.-J. (1996). "Kinetics of formation of monodisperse colloidal silica particles through the hydrolysis and condensation of tetraethylorthosilicate," *Industrial & Engineering Chemistry Research* 35(12), 4487-4493. DOI: 10.1021/ie9602217
- Chen, F., Gong, A. S., Zhu, M., Chen, G., Lacey, S. D., Jiang, F., Li, Y., Wang, Y., Dai, J., Yao, Y., *et al.* (2017). "Mesoporous, three-dimensional wood membrane decorated with nanoparticles for highly efficient water treatment," *ACS Nano* 11(4), 4275-4282. DOI: 10.1021/acsnano.7b01350
- Chen, C., Kuang, Y., Zhu, S., Burgert, I., Keplinger, T., Gong, A., Li, T., Berglund, L., Eichhorn, S. J., and Hu, L. (2020). "Structure property function relationships of natural and engineered wood," *Nature Reviews Materials* 5(9), 642-666. DOI: 10.1038/s41578-020-0195-z
- Deetz, J. D., Ngo, Q., and Faller, R. (2016). "Reactive molecular dynamics simulations of the silanization of silica substrates by methoxysilanes and hydroxysilanes," *Langmuir* 32(28), 7045-7055. DOI: 10.1021/acs.langmuir.6b00934
- Delley, B. (1990). "An all-electron numerical method for solving the local density functional for polyatomic molecules," *The Journal of Chemical Physics* 92(1), 508-517. DOI: 10.1063/1.458452
- Delley, B. (2000). "From molecules to solids with the DMol³ approach," *Journal of Chemical Physics* 113(18), 7756-7764. DOI: 10.1063/1.1316015
- Feng, L., Li, S., Li, Y., Li, H., Zhang, L., Zhai, J., Song, Y., Liu, B., Jiang, L., and Zhu, D. (2002). "Super-hydrophobic surfaces: From natural to artificial," *Advanced Materials* 14(24), 1857-1860. DOI: 10.1002/adma.200290020
- Hunsche, A., Görl, U., Müller, A., Knaack, M., and Göbel, T. (1997). "Investigations concerning the reaction silica/organosilane and organosilane/polymer. Part 1: Reaction mechanism and reaction model for silica/organosilane," *Kautschuk und Gummi Kunststoffe* 50(12), 881-889.
- Iarlori, S., Ceresoli, D., Bernasconi, M., Donadio, D., and Parrinello, M. (2001). "Dehydroxylation and silanization of the surfaces of β -cristobalite silica: An *ab initio* simulation," *The Journal of Physical Chemistry B* 105(33), 8007-8013. DOI: 10.1021/jp010800b
- Li, H., Chang, S., Li, Y., Guo, F., Xu, J., Zhang, Y., Li, H., and Shang, Y. (2022). "A soft and recyclable carbon nanotube/carbon nanofiber hybrid membrane for oil/water separation," *Journal of Applied Polymer Science* 139(19), 1-9. DOI: 10.1002/app.52133
- Li, T., Chen, C., Brozena, A. H., Zhu, J. Y., Xu, L., Driemeier, C., Dai, J., Rojas, O. J., Isogai, A., Wågberg, L., *et al.* (2021). "Developing fibrillated cellulose as a

- sustainable technological material,” *Nature* 590(7844), 47-56. DOI: 10.1038/s41586-020-03167-7
- Li, T., Liu, H., Zhao, X., Chen, G., Dai, J., Pastel, G., Jia, C., Chen, C., Hitz, E., Siddhartha, D., *et al.* (2018). “Scalable and highly efficient mesoporous wood-based solar steam generation device: Localized heat, rapid water transport,” *Advanced Functional Materials* 28(16), 1-8. DOI: 10.1002/adfm.201707134
- Liu, R., Xu, Y., Wu, D., Sun, Y., Gao, H., Yuan, H., and Deng, F. (2004). “Comparative study on the hydrolysis kinetics of substituted ethoxysilanes by liquid-state ^{29}Si NMR,” *Journal of Non-Crystalline Solids* 343(1), 61-70. DOI: 10.1016/j.jnoncrysol.2004.07.032
- Liu, M., Wang, S., and Jiang, L. (2017). “Nature-inspired superwettability systems,” *Nature Reviews Materials* 2(7), 1-17. DOI: 10.1038/natrevmats.2017.36
- Perdew, J. P., Burke, K., and Ernzerhof, M. (1996). “Generalized gradient approximation made simple,” *Physical Review Letters* 77(18), 3865-3868. DOI: 10.1103/PhysRevLett.77.3865
- Phat, L. N., Thang, T. Q., Nguyen, H. C., Duyen, D. T. M., Tien, D. X., Khoa, B. D. D., Khang, P. T., Giang, N. T. H., Nam, H. M., Phong, M. T., *et al.* (2021). “Fabrication and modification of cellulose aerogels from Vietnamese water hyacinth for oil adsorption application,” *Korean Journal of Chemical Engineering* 38(11), 2247-2255. DOI: 10.1007/s11814-021-0853-x
- Rana, A. K., Frollini, E., and Thakur, V. K. (2021). “Cellulose nanocrystals: Pretreatments, preparation strategies, and surface functionalization,” *International Journal of Biological Macromolecules* 182, 1554-1581. DOI: 10.1016/j.ijbiomac.2021.05.119
- Shang, Z., and Zhang, X. (2019). “DFT study on effects of hydrolysis degrees of 3-mercaptopropyltriethoxysilane on grafting mechanisms of nano-silica,” *CIESC Journal* 70(5), 1663-1673. DOI: 10.11949/j.issn.0438-1157.20180940
- Shang, Z., and Zhang, X. (2020). “Theoretical study on the interactions between silica and the products of 3-mercaptopropyltriethoxysilane (MPTS) with different hydrolysis degrees,” *Applied Surface Science* 502, 1-12. DOI: 10.1016/j.apsusc.2019.143853
- Shircliff, R. A., Stradins, P., Moutinho, H., Fennell, J., Ghirardi, M. L., Cowley, S. W., Branz, H. M., and Martin, I. T. (2013). “Angle-resolved XPS analysis and characterization of monolayer and multilayer silane films for DNA coupling to silica,” *Langmuir* 29(12), 4057-4067. DOI: 10.1021/la304719y
- Tu, H., Zhu, M., Duan, B., and Zhang, L. (2021). “Recent progress in high-strength and robust regenerated cellulose materials,” *Advanced Materials* 33(28), 1-22. DOI: 10.1002/adma.202000682
- Vilmin, F., Bottero, I., Travert, A., Malicki, N., Gaboriaud, F., Trivella, A., and Thibault-Starzyk, F. (2014). “Reactivity of bis[3-(triethoxysilyl)propyl] tetrasulfide (TESPT) silane coupling agent over hydrated silica: Operando IR spectroscopy and chemometrics study,” *The Journal of Physical Chemistry C* 118(8), 4056-4071. DOI: 10.1021/jp408600h
- Wang, X., Xu, S., Tan, Y., Du, J., and Wang, J. (2016). “Synthesis and characterization of a porous and hydrophobic cellulose-based composite for efficient and fast oil-water separation,” *Carbohydrate Polymers*, 140, 188-194. DOI: 10.1016/j.carbpol.2015.12.028
- Wang, K., Liu, X., Tan, Y., Zhang, W., Zhang, S., and Li, J. (2019). “Two-dimensional

- membrane and three-dimensional bulk aerogel materials via top-down wood nanotechnology for multibehavioral and reusable oil/water separation,” *Chemical Engineering Journal* 371, 769-780. DOI: 10.1016/j.cej.2019.04.108
- Xie, Y., Hill, C. A. S., Xiao, Z., Militz, H., and Mai, C. (2010). “Silane coupling agents used for natural fiber/polymer composites: A review,” *Composites Part A: Applied Science and Manufacturing* 41(7), 806-819. DOI: 10.1016/j.compositesa.2010.03.005
- Xie, Y., Xiao, Z., Militz, H., and Hao, X. (2017). “Silane coupling agents used in natural fiber/plastic composites,” in: *Handbook of Composites from Renewable Materials*, V. K. Thakur, M. K. Thakur, and M. R. Kessler (eds.), John Wiley & Sons, Ltd., Hoboken, NJ, pp. 407-430.
- Xing, T., Dong, C., Wang, X., Hu, X., Liu, C., and Lv, H. (2022). “Biodegradable, superhydrophobic walnut wood membrane for the separation of oil/water mixtures,” *Frontiers of Chemical Science and Engineering*, 1–10. DOI: 10.1007/s11705-022-2157-z
- Ye, D., Lei, X., Li, T., Cheng, Q., Chang, C., Hu, L., and Zhang, L. (2019). “Ultra-high tough, super clear, and highly anisotropic nanofiber-structured regenerated cellulose films,” *ACS Nano* 13(4), 4843-4853. DOI: 10.1021/acsnano.9b02081
- Yokoyama, A., Ohwada, T., and Shudo, K. (1999). “Prototype Pictet-Spengler reactions catalyzed by superacids. Involvement of dicationic superelectrophiles,” *The Journal of Organic Chemistry* 64(2), 611-617. DOI: 10.1021/jo982019e
- Yoshida, W., Castro, R. P., Jou, J.-D., and Cohen, Y. (2001). “Multilayer alkoxy silane silylation of oxide surfaces,” *Langmuir* 17(19), 5882-5888. DOI: 10.1021/la001780s
- Zhao, D., Zhu, Y., Cheng, W., Chen, W., Wu, Y., and Yu, H. (2021). “Cellulose-based flexible functional materials for emerging intelligent electronics,” *Advanced Materials* 33(28), 1-18. DOI: 10.1002/adma.202000619
- Zhu, H., Luo, W., Ciesielski, P. N., Fang, Z., Zhu, J. Y., Henriksson, G., Himmel, M. E., and Hu, L. (2016). “Wood-derived materials for green electronics, biological devices, and energy applications,” *Chemical Reviews* 116(16), 9305-9374. DOI: 10.1021/acs.chemrev.6b00225
- Zhu, M., Li, Y., Chen, G., Jiang, F., Yang, Z., Luo, X., Wang, Y., Lacey, S. D., Dai, J., Wang, C., *et al.* (2017). “Tree-inspired design for high-efficiency water extraction,” *Advanced Materials* 29(44), 1-9. DOI: 10.1002/adma.201704107
- Zhuo, L.-G., Liao, W., and Yu, Z.-X. (2012). “A frontier molecular orbital theory approach to understanding the Mayr equation and to quantifying nucleophilicity and electrophilicity by using HOMO and LUMO energies,” *Asian Journal of Organic Chemistry* 1(4), 336-345. DOI: 10.1002/ajoc.201200103

Article submitted: May 4, 2022; Peer review completed: June 4, 2022; Revised version received and accepted: August 9, 2022; Published: August 15, 2022.
DOI: 10.15376/biores.17.4.5728-5740